STUDIA UBB CHEMIA, LXVII, 1, 2022 (p. 107-124)
(RECOMMENDED CITATION)
DOI:10.24193/subbchem.2022.1.07

A NOVEL SCHIFF BASES/MULTIWALLED CARBON NANOTUBE BASED ADSORBENTS TO REMOVE ^{210}Pb FROM WATER

NAZIFE ASLAN[a*], ORHAN ATAKOL[b], NILGÜN ŞEN[c]

ABSTRACT. This work presents the development of new adsorbent materials to remove lead-210 (^{210}Pb) from water. Adsorbents were constructed from the carboxylated carbon nanotubes modified with N,N'bis(salicylidene)1,3-diaminopropane (LH2) Schiff Base and N,N'bis(salicylidene)1,3-diaminopropane-Cu(II) (CuL) complexes. Scanning electron microscopy (SEM) was used to characterize the morphological features of the adsorbents. The effects of pH, contact time, temperature, and Schiff base concentration on lead(II) absorption were investigated in order to optimize the experimental conditions. The adsorption capacity of the adsorbents was determined using atomic absorption spectrometry. Both adsorbents had high adsorption capabilities, with about 98.0% in the first 30 minutes of contact time. The adsorption processes were also in good agreement with the Langmuir isotherm and pseudo-second-order kinetic models. The adsorption of ^{210}Pb from the tap water sample confirmed the applicability of the proposed adsorbents, and the results were satisfactory.

Keywords: *Multiwalled carbon nanotube, ^{210}Pb removal, Schiff base, radioisotopes*

INTRODUCTION

As a natural result of developing technology, toxic metal pollution poses a threat to public health and natural life. Unlike organic pollutants, they are not biodegradable in the environment. Therefore, most of the toxic metals accumulate in biological organisms and cause serious diseases such as thyroid, neurological, autism, infertility and even death.

[a] *Ankara Hacı Bayram Veli University, Polatlı Science and Arts Faculty, Chemistry Department, Turkey*
[b] *Ankara University, Science Faculty, Chemistry Department, Ankara, Turkey*
[c] *Turkish National Police Academy, Institute of Forensic Sciences, Ankara, Turkey*
** Corresponding author: nazife.aslan@hbv.edu.tr*

Toxic metals from industrial and urban waste are the most common sources of contaminants in water and soil, and lead is one of the most dangerous. It must be carefully monitored for human health and environmental damage because it is both chemically hazardous and has a radioactive isotope [1,2]. Lead does not have a physiological role in the body. Its presence can lead to toxic effects in every organ system, regardless of age, gender, or exposure pathway. Of all the organs, the nervous system is most affected by lead toxicity, both in children and adults. The toxicity on children is, however, of a more significant impact than in adults. Prolonged exposure to lead is known to cause anemia with increased blood pressure [3-6].

The human body can discharge 1-2 mg of lead per day with regular functions. However, lead which is unable to be excreted from the body accumulates in the bones, liver, kidneys, and muscles, causing a variety of ailments such as hypertension, nausea, obesity, and behavioral disorders. It means that the 15 $\mu g.L^{-1}$ lead level in water set by the United States Environmental Protection Agency (EPA) is not a public health threshold, and that decreasing below it does not guarantee the water is safe [7].

Several separation techniques such as ion exchange, chemical precipitation, reverse osmosis, evaporation, membrane filtration, solvent extraction, biological absorption, and adsorption treatment have been reported recently [8-18]. The adsorption process offers several advantages over the others regarding rapid response, high sensitivity, and ease of preparation. As a result of these factors, there is a growing interest in developing new adsorbents to remove harmful metals as well as natural and anthropogenic radioisotopes from environmental samples. [19-20].

Nanotechnology is one of the most important trends in material science right now. Nanoparticles are also being investigated for application in the production of high-performance adsorbents. Carbon nanotubes (CNTs) demonstrate an essential group of nanomaterials. They have unique physical and chemical properties such as large specific surface area, high reactivity, high adsorption and desorption capacity, and low-temperature modification ability. These characteristics have enhanced the usage of carbon nanotubes in environmental technologies [21,22]. However, the insolubility of new generation carbon nanotubes in a variety of solvents restricts their use. In their natural form, carbon nanotubes are chemically inert, but they can be chemically modified with a variety of organic compounds. Thus, they are easy to interact with adsorbates and have greater maximum adsorption capacity after modification [23,24].

Modification can be achieved in two ways: covalent and non-covalent. The electrical structure of CNT is not damaged as a result of its non-covalent modification, which is one of its key advantages. CNTs can be modified using

oxidants such as photo-oxidation, oxygen plasma, or gas phase. On the other hand, the discovery of ultrasonic treatment with nitric and/or sulfuric acid as an oxidation technique, on the other hand, is a major turning point in CNT chemistry. Covalent modification of CNT walls in a systematic and controlled manner is also crucial for many CNT applications and is vital.

Schiff bases (SB) are azomethine-containing compounds, which were first synthesized by Hugo Schiff in 1864. They are condensation products of ketones (or) aldehydes with primary amines. Schiff base ligands can form stable complexes with various metal ions. This property improves their suitability as a novel adsorbent material for the removal of a number of hazardous metals and radioisotopes.

This work aimed to prepare new adsorbent materials for the rapid, sensitive, and practical removal of ^{210}Pb radioisotope from water. For this purpose, multiwalled carbon nanotube (MWCNT) surfaces are carboxylated (F-MWCNT) by an appropriate oxidation procedure and the adsorption of Schiff bases to the surface is provided. The obtained Schiff base-multiwalled carbon nanotube (SB/F-MWCNT) was characterized by scanning electron microscopy (SEM) analysis. Measurements focused on several adsorption parameters such as adsorption capacity, adsorption time, the influence of the Schiff base concentrations, pH of the solution, and temperature. Firstly, the experimental parameters that can affect the adsorption performance investigated using a non-radioactive Pb(II) solution, and optimum working conditions were determined. The results showed that these new adsorbents have a high adsorption capacity towards Pb(II) ions from aqueous solutions and encouraged us to use these materials for the removal of ^{210}Pb radioisotopes in water samples. The adsorption mechanism of lead(II) ions onto SB/F-MWCNT was evaluated thermodynamics and kinetics. For this, Freundlich and Langmuir adsorption isotherm models and kinetic parameters were derived using adsorption's experimental results.

It is known that there are many studies published in the literature concerning the removal of toxic lead(II) ions by using several adsorbents. But only a few works of literature were found about the removal of ^{210}Pb in drinking water. We think that the results of the study will make valuable contributions to the literature in this respect, too.

RESULTS AND DISCUSSION

Surface characterization studies of treated MWCNTs using SEM

SEM was used to obtain morphological images of modified carbon nanotubes. Figures 1a, 1b, and 1c show F-MWCNTs images before and after modification with LH2 and CuL, respectively. In Figures 1a, 1b, and 1c, we

can see some yarns that look just like fibers. The SEM analysis indicates that products have a tubular surface morphology. The modified carbon nanotube's morphological structure is not uniform, and there are white spots in the presence of clots. The white patches and dots are not representative of carbon nanotubes. When the images were compared, it was seen that the carbon nanotubes had an apparent thickening in their diameters. The source of this increase is the Schiff base, which adsorbs to the surface.

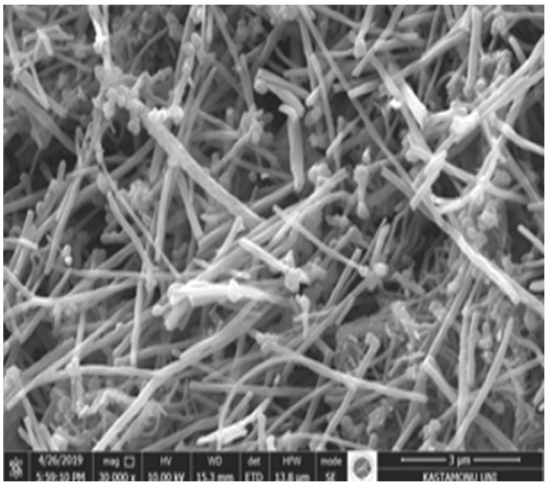

Figure 1a. SEM images of F-MWCNTs before the modification

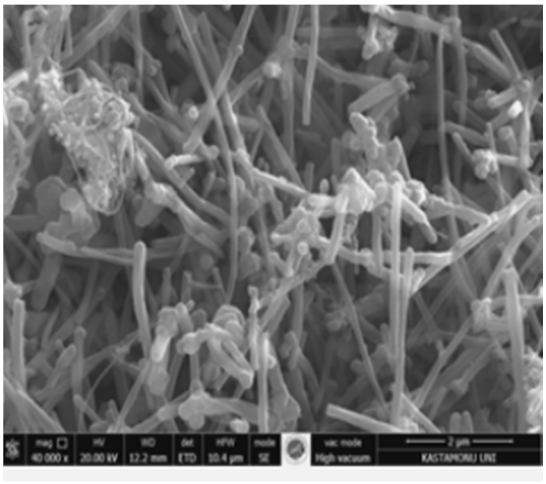

Figure 1b. SEM images of F-MWCNTs after the modification with LH2

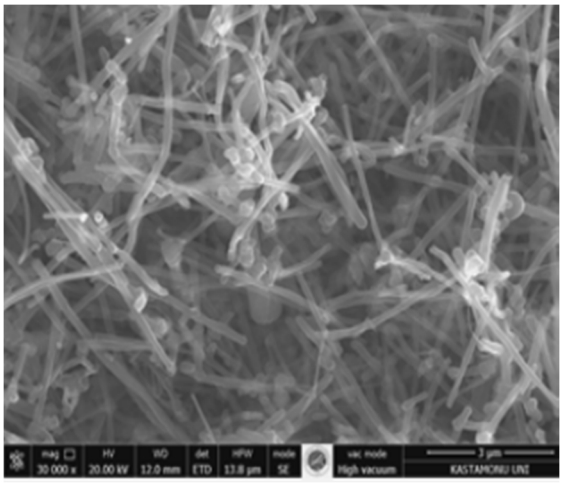

Figure 1c. SEM images of F-MWCNTs after modification with CuL

Effect of contact time

Contact time determination is one of the crucial parameters in the adsorption process. 2 $g.L^{-1}$ adsorbent and 20 $mg.L^{-1}$ lead(II) concentration are used to determine the equilibrium time in removing lead(II) ions with LH2/F-MWCNTs and CuL/F-MWCNTs at room temperature. As indicated in Figure 2, the contact time experiment was carried out for up to 120 minutes to see when the adsorption reached equilibrium. The adsorption of Pb(II) ions was rapid initially, but as contact time increased, it became slower until it reached equilibrium. The removal of lead (II) ions was particularly fast within the first 30 minutes of contact time because the adsorbents have many empty surface sites for adsorption. LH2/F-MWCNTs have a higher adsorption capacity than CuL/F-MWCNTs, as seen in the Figure 2.

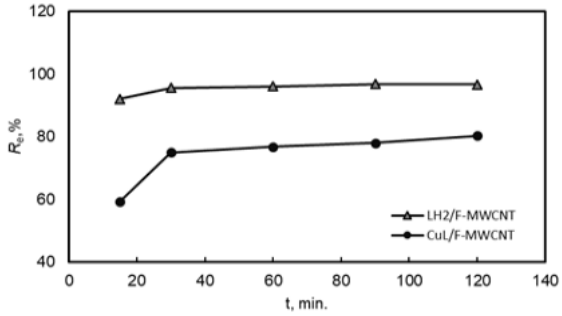

Figure 2. Effect of contact time on removal of Pb(II).

Effect of pH on adsorption

The pH value is significant parameter in the adsorption operations because adsorption capability is highly dependent on pH. When the pH of a solution changes, the adsorbent properties differ due to complex formation, hydrolysis, precipitation, and redox reactions in the solution.

An optimum pH was examined within a range of 2.0 – 7.0 in the 20 mg.L^{-1} initial Pb(II) concentration. Figure 3 shows that Pb(II) adsorption increases with pH until it reaches 6.0 and then decreases. The concentration of H^+ ions in the solution is high at low pH values, and lead ions exist in the form of Pb^{2+}. Lead ions compete with protons to diffuse onto adsorbent surfaces in this case [17]. Because the adsorbent surface is positively charged at low pH, it repels Pb(II) ions. The concentration of hydrogen ions competing with the lead(II) ions decrease as the pH of the solution increases, but the number of lead(II) ions adsorbed rises. Many researches have claimed that different adsorbents remove metal ions in the same way. [25-26].

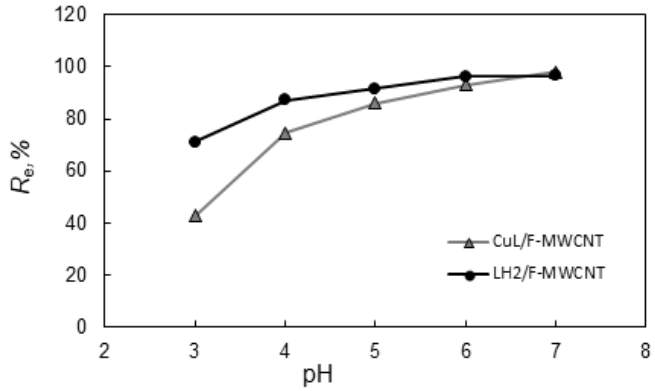

Figure 3. Effect of solution pH on the adsorption percentage of Pb^{2+} onto SB-F-MWCNT (M=2 g.L^{-1}; C_o=20 mg.L^{-1}, V=0.025 L, T=298 K, and adsorption period=30 min.).

Influence of initial Pb(II) concentration

Optimization of the initial metal concentration is another crucial parameter to achieve the best adsorption conditions. At a constant SB/F-MWCNT concentration of 2 g.L^{-1}, the effect of the initial Pb(II) concentration on adsorption behavior was examined between 5.0 - 30.0 mg.L^{-1}. Table 1 presents the outcomes of the experiments. LH2/F-MWCNT and CuL/F-MWCNT had a maximum adsorption efficiency of 99.5% and 84.3%, respectively.

Table 1. The effect of initial Pb (II) concentration on the adsorption efficiency.

	R_e , %	R_e, %	q_e, mg.g^{-1}	q_e, mg.g^{-1}
C_o, mg.L^{-1}	LH2/F-MWCNT	CuL/F-MWCNT	LH2/F-MWCNT	CuL/F-MWCNT
5	88.6	56.3	2.63	2.01
10	92.0	74.1	4.85	4.15
15	97.9	81.1	6.25	6.01
20	99.5	84.3	8.72	8.14
30	95.5	83.6	13.8	13.1

Since the adsorbent surface has a sufficient number of binding sites to which the metal can bind, the adsorption efficiency will initially increase as the metal concentration increases.

When the lead(II) concentration exceeds 20 mg.L^{-1}, however, the adsorption efficiency decreases, as seen in Figure 4. After 20 mg.L^{-1}, the adsorbent surface to which the metal will bind decreases due to the saturation of empty centers.

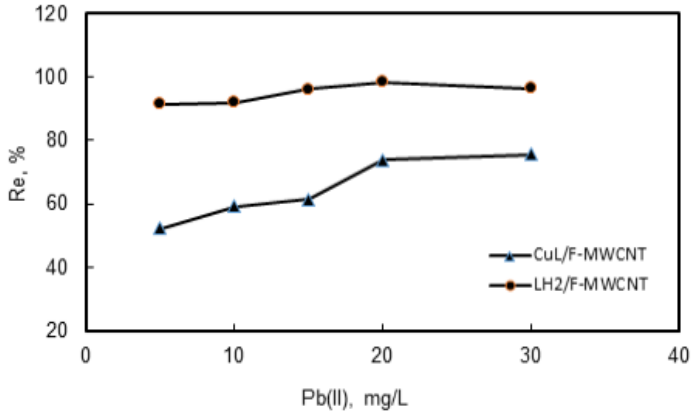

Figure 4. Effect of initial Pb(II) concentration on the adsorption efficiency.

Effect of Schiff base dosage

One of the most critical parameters determining the metal ions' adsorption rate from an aqueous solution is the adsorbent quantity. The effect of changing the Schiff base concentration (0.1% - 0.3% (w/v)) was investigated. When the amount of adsorbents was increased from 0.1% to 0.3%, the percentage of Pb(II) removed increased from 93.2 to 98.8% and

71.4 to 84.2% for LH2/F-MWCNT and CuL/F-MWCNT, respectively. By increasing the amount of adsorbent, the bonding groups available on the adsorbent surface increase and provide more adsorption sites for the Pb(II) ions. Thus, an increase in metal ion uptake occurs. However, there was no significant increase in the percentage removal for both adsorbents after the 0.2% (w/v) dosage. Thus, each Schiff base optimum concentration is considered to be 0.2% and used in further experiments.

The effect of temperature

For some adsorbents, temperature can have a significant impact on the adsorption process. Therefore, the effect of temperature on Pb(II) adsorption was investigated at 20°C, 30°C, and 40°C (Figure 5). As seen in the Figure 5, temperature has a minor effect on the adsorption capabilities of both adsorbents. The adsorption capacities of LH2/F-MWCNT and CuL/F-MWCNT decreased from 8.25 mg/g to 7.96 mg/g and from 8.09 mg/g to 7.58 mg/g, respectively, with the increase in temperature from 20 °C to 40 °C.

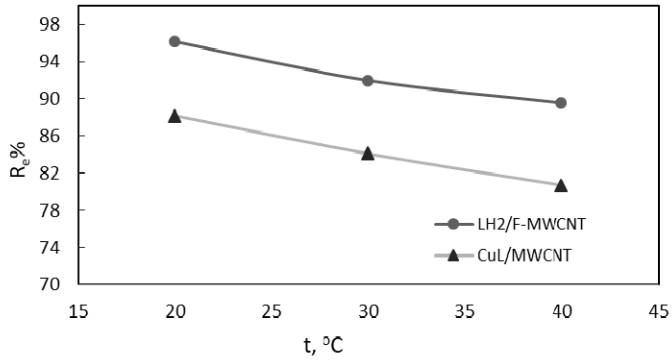

Figure 5. Temperature effects on the removal of Pb (II) ions onto (•) LH_2/F-MWCNTs and (∆) CuL/F-MWCNTs.

Adsorption kinetics

To examine the kinetic parameters affecting the adsorption of lead(II) onto LH2/F-MWCNT and CuL/F-MWCNT, contact times were varied from 0 to 120 minutes. The relationships between t and t/qt were plotted according to the experimental values (Figure 6). The data was then used to create pseudo-first and pseudo-second-order models. The intercepts and slopes of the linear plots were used to calculate the pseudo-first and pseudo-second-

order constants k_1 and k_2, as well as the equilibrium capacity q_e. The q_e value calculated from the pseudo-first-order kinetic model is considerably lower than the experimental data. The q_e value of the pseudo-second-order kinetic model, on the other hand, is closer to the experimental q_e value (Figure 6, Table 2). The obtained R2 values also indicate that the correlation for both adsorbents is extremely high. Based on these findings, we may conclude that the adsorption behavior of this system is consistent with the pseudo-second-order kinetic model.

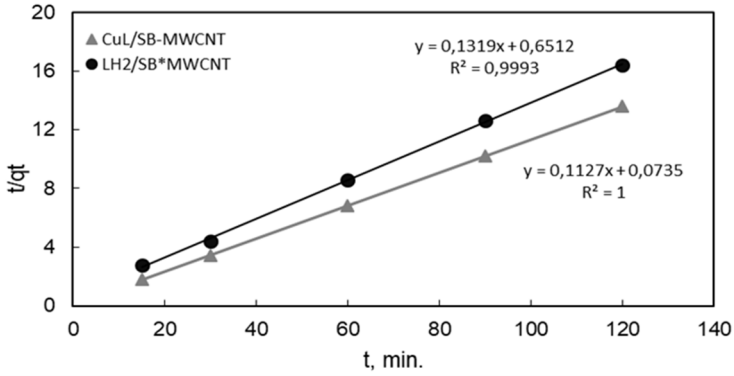

Figure 6. Pseudo-second-order kinetic of Pb(II) adsorption on SB/F-MWCNT (M=2 g.L^{-1}, C_o=20 mg.L^{-1}, V=0.025 L, T=298 K, and adsorption period=30 min.)

Table 2. Kinetic parameters of pseudo-second-order equations for Pb(II) adsorption onto SB/F-MWCNT at 20 mg.L^{-1}

Adsorbents	q_e-exp. (mg.g^{-1})	q_e-calc. (mg.g^{-1})	k_2 (g.mg^{-1}.min^{-1})	R^2
LH2/F-MWCNT	8.713	8.873	0.1728	0.9993
CuL/F-MWCNT	7.066	7.582	0.0267	1.0000

Adsorption isotherms

At a constant temperature, the adsorption isotherm describes the relationship between concentration and the amount of substance adsorbed by the adsorbent. For the study of equilibrium data, developing an equation that can be used to optimize experimental circumstances is critical. In wastewater treatment applications, the Langmuir and Freundlich isotherm models have been widely used [27]. Plotting Langmuir and Freundlich isotherm curves explained the adsorption behavior of LH2/F-MWCNT and CuL/F-MWCNT against rising Pb(II) initial concentrations.

The equilibrium Pb (II) concentration was taken into account in isotherm experiments, and the isotherm constants were calculated using Equation 6-8. The linearized Langmuir and Freundlich isotherms were used to determine the adsorption capacities of LH2/F-MWCNT and CuL/F-MWCNT for lead (II) ions, as seen in Table 3.

Table 3. Langmuir and Freundlich isotherm parameters for Pb(II) adsorption onto SB/F-MWCNT

	Langmuir constants			Freundlich constants			
.Adsorbents	q_m, mg.g^{-1}	K_L, L.mg^{-1}	R^2	1/n	n	K_f, (mg/g)(L/mg)$^{1/n}$	R^2
LH2/F-MWCNT	7.95	31.44	0.992	0.476	2.10	8.31	0.787
CuL/F-MWCNT	4.35	0.358	0.949	0.408	2.45	0.683	0.875

The data in Table 3 shows that the R^2 values of the two isotherm models were reasonably suitable for describing the adsorption. However, the Langmuir equation provided a better fit than the Freundlich equation. The determination coefficients (R^2) show that the adsorption data for Pb(II) best fit the Langmuir isotherm for both adsorbents. LH2/F-MWCNT has a better adsorption capacity (q_m) than CuL/F-MWCNT.

For comparison, Table 4 summarizes the adsorption capabilities of adsorbents previously described in the literature. The highest adsorption capacity, q_m (mg.g^{-1}), determined in this study was in good conformity with those reported in the literature. However, differences in adsorbent properties like structure, surface area, porosity, and functional groups could explain the variations in adsorption capabilities.

Table 4. Comparison of the adsorption capacity of various adsorbents for Pb(II)

Adsorbents,	q_m (mg.g^{-1})	Adsorption Conditions				
		pH	t (°C)	C_0 (mg.L^{-1})	Adsorbent Dosage (g.L^{-1})	Ref
Polypyrrole-based AC	50.0	5.5	23	100	5.0	[2]
Acidified CNTs	17.44	5.0	-	10	-	[12]
PPyo/MWCNT composite	26.32	6.0	25	10 - 100	1.0	[36]
Activated C	21.38	6.0	20 ± 2	10 - 100	0.2 - 2	[38]
SB/F-MWCNT	40.69	6.0	25	20	2.0	This work

Real sample application of the adsorbents
Removal of ^{210}Pb radioisotope in spike tap water

The main purpose of this study was to develop new adsorbents for removing ^{210}Pb from water using multiwalled carbon nanotube modified with Schiff bases. The radioactive and non-radioactive isotopes of a metal ion have identical chemical characteristics. As a result, the best adsorption conditions were first identified using a non-radioactive lead(II) solution. After that, the real-sample applications of the developed adsorbents were made in tap water samples spiked with ^{210}Pb reference solution. To achieve this, a standard reference ^{210}Pb solution with about 25 Bq activity was added to a tap water sample containing 2 g.L^{-1} of adsorbent at pH 6.0.

Liquid Scintillation Spectrometry (LSS) was used to determine both the added and measured activity concentrations of ^{210}Pb, and the results are shown in Table 5.

Table 5. Removal of ^{210}Pb from tap water using LH2/F-MWCNT and CuL/F-MWCNT adsorbents (V = 0.025 L, t = 25 ° C and adsorption time = 30 min.).

Sample code	Adsorbent mass, (g)	Added activity, Bq	Measured activity, Bq	Adsorption efficiency, %
LH2/F-MWCNT	0.0505	27.89	0.09	99.7
CuL/F-MWCNT	0.0505	22.98	0.09	99.6

After only 30 minutes of adsorption, the proposed adsorbents can remove almost all of the ^{210}Pb isotopes. These results support the use of LH2/F-MWCNT and CuL/F-MWCNT to control the quality of drinking water in radiological emergencies.

CONCLUSIONS

Our research is divided into two parts: adsorption condition optimization and real sample applications. Batch experiments were performed with two new adsorbents developed using N,N'bis(salicylidene)1,3-diaminopropane Schiff Base and N,N'bis(salicylidene)1,3-diaminopropane-Cu(II) complexes modified with MWCNT-COOH. In terms of radiation protection, the outcomes of the study indicate that both adsorbents developed can successfully remove ^{210}Pb from drinking water in a short period of time with a high adsorption efficiency.

EXPERIMENTAL SECTION

Materials and methods

Reagents and solutions

All materials and chemicals were of analytical grade and used without further purification. The 18.2 mΩ deionized water needed throughout the study was obtained from pure water equipment Millipore, Milli-Q A-10 (Darmstadt, Germany). Hydrochloric (37%, Merck) acid and nitric acid solutions (≥69%, Fluka), used for the pH adjustment, were prepared by diluting concentrated solutions. Multiwalled carbon nanotube (MWCNT; D × L = 110–170 nm × 5–9 μm) obtained from Sigma Aldrich (Milwaukee, WI, USA). In the modification of the adsorbents, Triton X-100 (Fluka) was used. The standard solution of 1000 ± 2 mg/L Pb(II) was purchased from ORION (94-26-06). Again, this standard solution was diluted with ultrapure water to obtain the relevant initial concentrations of Pb(II) working solutions. HNO_3 or NaOH was used to change the initial pH of the solutions.

The ^{210}Pb standard solution was used, with a reference date of June 15, 2019, and an activity concentration of 7.467 $kBq.g^{-1}$ (Eckert and Ziegler Isotope Products, catalog number 7210). , A working standard solution with 27.96 $Bq.g^{-1}$ was prepared by diluting this reference solution in 1 M HNO_3. A quench set with a tritium (^3H) activity concentration of 7.385 kBq/g was prepared using a certified reference solution from Eckert and Ziegler Isotope Products (reference date is August 1, 2009, and Source No: 7003). A High-capacity Ultima Gold cocktail was used as a scintillator.

Instrumentation and measurements

All atomic absorption measurements were carried out with a flame atomic absorption spectrophotometer with a deuterium lamp (BGC-D2) (FAAS) (PinAAcle 900T, PerkinElmer, Waltham, MA, USA) and an automatic data processor. An acetylene-air flame was used for the determination of lead by FAAS.

Scanning Electron Microscope images were obtained using SEM from Thermo Fischer FEI Quanta FEG 250. The pH of the solutions was measured using an Orion Model 720A pH/ion meter and a combined pH electrode.

The Wallac 1220 Quantulus ultra low-level liquid scintillation spectrometer was used to measure beta radiation of ^{210}Pb. The efficiency of the instrument was calculated with the CIEMAT/NIST tritium efficiency tracing method. [28,29]. For this purpose, a standard tritium solution with known activities was put into low diffusion polyethylene vials, and 0 to 200 μL nitromethane was added

as a quenching agent. The dependence of the ^{3}H counting efficiency on the quench parameter (SQP[E]) was measured experimentally. Combining the theoretical and experimental quench curves allowed for calculating the efficiency of ^{210}Pb using the C/N 2005 program (E. Gunther, PTB/Latest version August 2005). 20 mL Teflon coated low diffusion polyethylene vials (Perkin Elmer) were used for counting the samples. To obtain a homogeneous mixture, the sample vials were sealed and shaken. The counting window was set to channels 1–1024 in the C/N methods. The activity of non-adsorbed ^{210}Pb radioisotopes remaining in the solution was determined using EASY View Spectrum Analysis Software.

Functionalization of MWCNT

Raw–MWCNT (2.0 g) with a purity of >95% was dispersed in 50 mL of concentrated HNO_3. Then the mixture was refluxed for 6 h at 140 ºC to produce oxidized carbon nanotubes MWCNT-COOH (F-MWCNT). The samples were filtered and washed with deionized water several times until neutral pH was reached, finally dried in a vacuum oven at 100ºC for 24 h.

Preparation of the adsorbents (Schiff Base/F-MWCNT)

The modification of functionalized carbon nanotubes was made using Triton X-100 and two Schiff bases synthesized previously in our laboratory. These Schiff bases were called N,N'bis(salicylidene)1,3- diaminopropane and N,N'bis(salicylidene)1,3-diaminopropane-Cu (II), respectively (Figure 7a and Figure 7b).

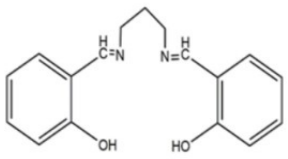

Figure 7a. N,N 'bis(salicylidene) 1,3 diaminopropane.

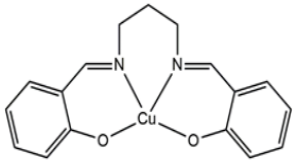

Figure 7b. N,N' bis (salicylidene) 1,3 diaminopropane-Cu (II)

The modification was made according to the following procedure. 50 mL of a 0.2 percent (w/v) methanol solution of each LH2, CuL, and 0.4 g of Triton X-100 were added to 200 mg of functionalized carbon nanotube. The mixture was first sonicated in an ultrasonic bath for 4 hours and then stirred on a magnetic stirrer for 12 hours. The Schiff bases adsorbed on functionalized multiwalled carbon nanotube (SB/F-MWCNT) was vacuum filtered and dried at room temperature. Two different adsorbent materials were prepared using Schiff bases bound to CNT surfaces at the end of this process. Triton X-100 helped the physical adsorption of Schiff bases onto the CNT surfaces and increased the dispersing ability of adsorbent materials.

Characterization of F-MWCNTs and SB/F-MWCNT

The surfaces of functionalized carbon nanotubes (F-MWCNTs) were examined with a Scanning Electron Microscope (Thermo Fischer FEI Quanta FEG 250 SEM) with 1.2 nm resolution before and after modification with CuL and LH2 Schiff bases.

Adsorption experiments

By diluting an accurately measured stock $Pb(NO_3)_2$ solution in deionized water, a working solution with a concentration of 100 mg/L was prepared. Different Pb(II) concentrations were obtained by diluting the working solution with deionized water. For all experiments, freshly produced solutions were used. The adsorption studies were carried out in a glass beaker at room temperature. To begin, 50.0 mg of adsorbent and 25 mL of known concentration of Pb (II) were taken into a glass beaker and mixed with a magnetic stirrer at a constant stirring speed of 150 rpm. Following adsorption, a 1.0 mL sample solution was taken from the exact part of the reaction mixture at predetermined intervals. FAAS was used to measure Pb(II) concentrations. According to the results, both of the novel adsorbents efficiently adsorbed the lead(II) ions from the water sample. The effect of parameters including pH, contact time, and adsorbent quantity on the adsorption behavior of the adsorbents was also examined. One parameter was changed and studied for each case, while the other parameters remained constant.

50.0 mg of SB/F-MWCNT was mixed with 25 mL of Pb(II) ion solution to evaluate the kinetic mechanism of the adsorption process. The initial lead(II) ion concentration was changed from10 $mg.L^{-1}$ to 30 $mg.L^{-1}$. To adjust the pH of the solutions, 0.100 M HNO_3 and 0.100 M NaOH solutions were prepared. The difference between the initial and equilibrium Pb(II) concentrations of the solutions was used to calculate the amount of lead(II) ion adsorbed on the adsorbents during the given time intervals (0, 15, 30, 60, 90, and 120 minutes). At least three replicates were averaged for each measurement.

Theoretical calculations

Due to its simplicity, the adsorption of lead was studied by batch operation at room temperature. The Pb(II) ion concentration before and after adsorption was determined using flame atomic absorption spectrometry. The adsorbed amount of lead ions onto the LH2/F-MWCNT and CuL/F-MWCNT adsorbents was calculated according to the following Equations:

$$q_e = (C_0 - C_{eq}) \times \frac{V}{m} \quad (1)$$

$$R_e\% = \frac{(C_0 - C_{eq})}{C_0} \times 100 \quad (2)$$

where C_0 (mg/L) is the initial Pb(II) ion concentration, and C_{eq} (mg/L) is the concentration of Pb(II) after adsorption for particular time intervals. m denotes the adsorbent mass used in adsorption (g), and V denotes the volume of the solution (L).

The distribution coefficient, K_d (mL.g^{-1}), was calculated using Equation 3:

$$K_d = \frac{(C_0 - C_{eq})}{C_{eq}} \times \frac{V}{m} \quad (3)$$

Adsorption kinetics

Adsorption is a time-dependent process. Knowing the adsorption rate is essential in terms of both design and investigation of adsorbent usability. To do this, various equilibrium and kinetics analyses are used. The Langmuir and Freundlich isotherm models were used to analyse the results obtained for examining the adsorption equilibrium conditions. The adsorption kinetics of the SB/F-MWCNT adsorbent were investigated using pseudo-first-order [30] and pseudo-second-order [31] models. The Pseudo-first-order model, based on the adsorbent capacity, is given in Equation 4:

$$\log(q_e - q_t) = \log(q_e) - \frac{k_1 t}{2.303} \quad (4)$$

This kinetic model's applicability is possible if the plot of log (q_e) versus t gives a straight line. The q_e and k_1 values can be calculated from the slope of the line and the y-axis intercept. However, this model is not applicable for the total adsorption time in most cases; it is generally applicable for the first 20-30 minutes of the adsorption process.

The Pseudo second-order kinetic model is also a model based on the adsorbent capacity. The adsorption process considers the chemical adsorption mechanism. Unlike the first-order kinetic model, this model predicts behavior over the entire adsorption period [32,33]. The second-order kinetic model is represented by Equation 5:

$$\frac{t}{q_t} = \frac{1}{k_2\, q_e^2} + \frac{t}{q_e} \tag{5}$$

Where, k_2 is the second-order adsorption constant (g/mg.min). The *t/qt* values were plotted against the *t* to determine k_2 and q_e.

Adsorption isotherms

Adsorption is similar to an equilibrium reaction. When the solution comes into contact with a certain amount of adsorbent, the adsorbed material concentration decreases until it reaches equilibrium with those on the adsorbent surface. After the adsorption equivalence is established, the adsorbed substance's concentration in the solution phase remains constant. The amount of substance adsorbed by the adsorbent's unit mass is a function of temperature, concentration, pressure, or equilibrium pressure.

There are some mathematical models suggested for adsorption isotherms. Freundlich and Langmuir's isotherms are used more than other isotherms. In the Langmuir isotherm, assumptions are made that the adsorbed molecules on the surface are adsorbed as a single layer. The adsorption energy is the same all over the surface. There is no interaction between them the molecules attached to the surface [34]. The following Equation expresses the Langmuir isotherm;

$$\frac{\mathbf{1}}{\mathbf{q_e}} = \frac{\mathbf{1}}{\mathbf{q_m}} + \frac{1}{\mathrm{K_L q_m} C_e} \tag{6}$$

where q_m (mg/g) is the maximum adsorption capacity of the adsorbent (constant) and K_L (L/mg) is the Langmuir adsorption constant. Langmuir isotherm can be determined by plotting $1/q_e$ versus $1/C_e$.

Freundlich's model applies to adsorption on heterogeneous surfaces. It describes an empirical relationship that explains the adsorption of solutes from a liquid to a solid surface and the exponential distribution of active fields and energies [35,36].

$$q_e = K_F C_e^{1/n} \tag{7}$$

The logarithmic form of Equation 7 becomes

$$\log q_{\mathrm{e}} = \log K_{\mathrm{F}} + \frac{1}{\mathrm{n}} \log C_{\mathrm{e}} \quad (8)$$

K_{f} is the Freundlich constant related to the multilayer adsorption capacity, and n is the heterogeneity factor. The n parameter determine the type of process. If n = 1, the process is linear; if n > 1, the process is chemical; if n <1, the process is physical [37,38].

ACKNOWLEDGMENTS

The authors thank the Turkish Atomic Energy Authority, Sarayköy Nuclear Research, and Training Center, Liquid Scintillation Spectrometry Laboratory for the radioactivity measurements of the samples.

REFERENCES

1. B.M.W.P.K. Amarasinghe; R.A. Williams; *Chem. Eng. J.* **2007**, *32,* 299-309
2. N.R. Axtell; S.P.K. Sternberg; K.C. Laussen; *Bioresour. Technol.* **2003**, *89,* 41-48
3. A.L. Wani; A. Ara; J.A. Usmani; *Interdiscip. Toxicol*. **2015**, *8(2)*, 55-64
4. WHO/FAO/IAEA, Trace Elements in Human Nutrition and Health. Switzerland: Geneva, **1996**, 22-25.
5. A.D. Woolf, R. Goldman and D.C. Bellinger, *Pediatr. Clin. North. Am.* **2007**, *54,* 271-294.
6. A. Anjum; P. Lokeswari; M. Kaur; M. Datta; *J. Anal. Sci. Methods Instrum.* **2011**, *1(2),* 25-80.
7. EPA, United States Environmental Protection Agency, News Releases from Headquarters Water (OW). “EPA Proposes Updates to Lead and Copper Rule to Better Protect Children and At-Risk Communities”, 10.10.2019.
8. A. Anjum; *Sustainable Heavy Metal Remediation*, **2017**, *2,* 25-30.
9. C.K. Ahn; D. Park; S.H. Woo; J.M. Park; *J. Hazard. Mater.* **2009**, *164(2-3),* 1130-1136.
10. G. Issabayeva; M.K. Aroua; N. Meriam; N. Sulaiman; *J. Hazard. Mater*. **2008***, 155(1-2)*, 109-113.
11. T.A. Kurniawan; Y.S. Chan Gilbert; W.H. Lo; S. Babel; *Chem. Eng. J.* **2006**, *118***,** 83-98.
12. D.W. O’Connell; C. Birkinshaw; T.F. O’Dwyer; *Bioresour. Technol.* **2008***, 99***,** 6709-6724.

13. I.A. Elmaksod; S.A. Kosa; H. Alzahrani; E. Hegazy, *Egypt. J. Chem.* **2019***, 62(11)*, 2119-2129.
14. A. Agrawal; K.K. Sahu; B.D. Pandey; *Colloids and Surfaces A: Physicochem. Eng. Aspects,* **2004***, 237,* 133-140.
15. M. Ghaedi; E. Asadpour; A. Vafaie; *Spectrochim. Acta Part A: Molecular and Biomolecular Spect.* **2006**, *63(1)*, 182-188.
16. Y. Liang; X.H. Zhao; Q.M. Li; F.L. Cui; G.G. Liu; *Chinese J. Chem.* **2007**, *25(4)*, 521-526.
17. G. Issabayeva, M.K. Aroua and N.M.K. Sulaiman, Bioresour. Technol. **97***,* 2350 (2006).
18. M.A. Olatunji; M.U. Khandaker; Y.M. Amin; H.N.M.E. Mahmud; *Plos One*, **2016**, *11(10)*, 1-14.
19. M.A. Olatunji; O.B. Uwatse; M.U. Khandaker; Y.M. Amin; G. Faruq; *Royal Swedish Academy of Sciences, Physica Scripta*, **2014***, 89(12),* 125002-125008.
20. N.A. Kabbashi; M.A. Atieh; A. Al-Mamun; M.E.S. Mirghami; M.D.Z. Alam; N. Yahya, *J Environ. Sci.* **2009***, 21,* 539-544.
21. S. A. Kosa; G. Al-Zhrani; M. A. Salam; *Chem. Eng J.* **2012***, 181-182,* 159-164.
22. Q. Li; J. Yu; F. Zhou; X. Jiang; *Colloids Surf A: Physicochem. Eng. Aspects,* **2015***, 482,* 306-314.
23. M. Abdel Salam; G. Al-Zhrani; S.A. Kosa; *Comptes Rendus Chimie*. **2012***, 15(1-3)*, 398-408.
24. V.K. Gupta; S. Agarwal; T.A. Saleh; *Water Research,* **2011**, *45(6)*, 2207-2212.
25. M. Mohapatra; S. Anand; *J. Hazard. Mater.* **2007***, 148(3),* 553-559.
26. L. Mouni; D. Merabet; A. Bouzaza; L. Belkhiri; *Desalination,* **2011***, 276,* 148-153.
27. M.R. Matsumoto; *Sep. Sci. Technol.* **1993***, 28(13–14),* 2179-2186.
28. A.G. Malonda; E. Garcia-Toraño; J.M. Los Arcos, *Int. J Appl. Radiat. Isot.,* **1985**, *36,* 157-157.
29. A.G. Malonda; E. Garcia-Toraño; *Int. J Appl. Radiat. Isot.* **1982***, 33,* 249-253.
30. S. Lagegren; B. Svenska, *Vetenskapsakademiens Handlingar*, **1898***, 24*, 1-39.
31. Y.S. Ho; G. McKay, *Process. Biochem.* **1999***, 34(5)*, 451-465.
32. J. Guo; Y. Song; X. Ji; L. Ji; L. Cai; Y. Wang; H. Zhang; W. Song, *Materials,* **2019***, 12(2),* 241-258.
33. K. Mohanty; M. Jha; B. Meikap; M. Biswas, *Chem. Eng. Sci.* **2005***, 60(11),* 3049-3059.
34. I. Langmuir; *J. Am. Chem. Soc.* **1918***, 40,* 1361-1403.
35. H. Freundlich; *J. Phy. Chem.* **1906**, *57,* 1100-1107.
36. L. Wang; J. Zhang; R. Zhao; Y. Li; C. Li; C. Zhang; *Bioresour. Technol.* **2010***, 101(15),* 5808-5814.
37. A. Özer; H.B. Pirincci; *J. Hazard. Mater.* **2006***,137(2),* 849-855.
38. M.A. Hashem; *Int. J Phys. Sci.* **2007**, *2(7),* 178-184.